Wannier Koopman method calculations of the band gaps of alkali halides

Mouyi Weng, Sibai Li, Jie Ma, Jiaxin Zheng, Feng Pan, and Lin-Wang Wang

Citation: Appl. Phys. Lett. **111**, 054101 (2017); doi: 10.1063/1.4996743
View online: http://dx.doi.org/10.1063/1.4996743
View Table of Contents: http://aip.scitation.org/toc/apl/111/5
Published by the American Institute of Physics

Wannier Koopman method calculations of the band gaps of alkali halides

Mouyi Weng,[1,a)] Sibai Li,[1,a)] Jie Ma,[2] Jiaxin Zheng,[1] Feng Pan,[1,b)] and Lin-Wang Wang[3,b)]
[1]*School of Advanced Materials, Peking University, Shenzhen Graduate School, Shenzhen 518055, People's Republic of China*
[2]*School of Physics, Beijing Institute of Technology, Beijing 100081, China*
[3]*Materials Science Division, Lawrence Berkeley National Laboratory, Berkeley, California 94720, USA*

(Received 2 May 2017; accepted 17 July 2017; published online 31 July 2017)

Correcting the band structure within the density functional theory (DFT) formalism is a long term goal for its development. Recently, we have proposed a Wannier Koopman method (WKM) to correct the DFT bandgap using the Kohn-Sham equation. Previous tests show that WKM works well for common semiconductors. Here, we test its accuracy in terms of predicting the bandgap of extreme ionic crystals: alkali halides. We found that the WKM can accurately reproduce the alkali halide bandgaps with accuracy in par with the GW method. On the other hand, the hybrid functional with common parameters, which work well for common semiconductors, significantly underestimate the alkali halides. *Published by AIP Publishing.* [http://dx.doi.org/10.1063/1.4996743]

One of the long standing problems in the density functional theory (DFT) is its underestimation of the bandgaps using its Kohn-Sham orbitals eigen energies.[1] Many new exchange correlation functionals have been developed to solve this, along with many other problems, in the original functionals like the local density approximation (LDA)[2] or generalized gradient approximation (GGA).[3] These functionals are divided into semilocal functionals, like the meta-GGA[4] or the recently developed strongly constrained and appropriately normed (SCAN),[5,6] and the nonlocal hybrid functionals like B3LYP[7,8] or HSE[9] which include the explicit exchange integral. Some of these functionals focus on improving the ground state energies (e.g., SCAN), while there is no improvement for the bandgap problem, other functionals (like B3LYP, HSE, or meta-GGA[10]) also improve the bandgaps. But for the bandgap correction, the exact amount of correction might depend on the parameters. For the nonlocal hybrid functionals which incorporate part of the Fock exchange integral, the correction depends sensitively on how much the Fock exchange term is included. Very often, different types of materials might need drastically different parameters. Another approach to calculate the bandgap is the many body perturbation GW method.[11] However, it is shown that the G_0W_0 method might depend sensitively on the input wave functions and eigen energies.[12] On the other hand, there are many different self-consistent GW approaches, but the full self-consistent GW calculation yields bandgaps much larger than the experimental results.[13] Besides, the GW calculation is far more expensive than the DFT calculation, and it is also not directly connected to the DFT ground state total energy.

Given the above situation, it is thus worthwhile to continue to develop and test new methods which are based on DFT formalism, while correcting the current DFT bandgap error. Recently, we have presented a Wannier Koopman Method (WKM) to calculate the bandgap of crystals.[14] This method extends the widely known ΔDFT method of atom and small molecule calculations.[15] In ΔDFT, the electron affinity (EA) is calculated as E(N + 1)-E(N), while the ionization energy (IE) is calculated as E(N)-E(N-1), where N is the number of electron of the neutral system and E is the ground state total energy. While ΔDFT yields rather accurate EA, IE energies for molecules and atoms, in par with its ground state total energy accuracy, the same procedure applied to the extended bulk will yield the Kohn-Sham eigen energy due to Janak's theory.[16] This is because when one electron is added to the extended state, its charge density is infinitely small at any given spatial point, resulting in Janak's theory. In the WKM, instead of adding one electron to the extended states [like the conduction band minimum (CBM) and valence band maximum (VBM)], we will add the electron to the Wannier functions; thus, its charge density is not infinitely small locally, and hence, there will be a finite correction. More specifically, the total energy in the WKM is written as

$$E_{WKM} = E_{LDA} + \sum_w E_w(s_w). \tag{1}$$

Here, index "w" denotes the orthogonal Wannier functions in the occupied manifold or unoccupied manifold, $0 < s_w < 1$ is the occupation number of this Wannier function, and an analytical $E_w(s_w)$ term is added to ensure that E_{WKM} satisfies the Koopman theory for the Wannier function occupation number s_w: the value of E_{WKM} as a function of s_w is linear. The analytical expression of $E_w(s_w)$ is

$$E_w(s_w) = \lambda_w s_w(1 - s_w). \tag{2}$$

As $s_w = \sum_i \langle \phi_w | \psi_i \rangle^2 o(i)$, where ϕ_w is the Wannier function and ψ_i is the Kohn-Sham orbital, the modified Kohn-Sham equation can be obtained by taking a derivative of E_{WKM} with regard to ψ_i. We thus have

$$\left[H_{LDA} + \sum_w \lambda_w |\phi_w\rangle\langle\phi_w| \right] \psi_i = \varepsilon_i \psi_i. \tag{3}$$

Here, $\lambda_w = dE_w(s_w)/ds_w|_{s_w=0/1}$, $s_w = 0$ for the conduction band (since the conduction band is at $s_w = 0$ for conduction

[a)]M. Weng and S. Li contributed equally to this work.
[b)]Authors to whom correspondence should be addressed: panfeng@pkusz.edu.cn and lwwang@lbl.gov

band w) and $s_w = 1$ for the valence band (since the valence band is at $s_w = 1$ for valence band w). In order to calculate λ_w, we need to calculate $E_{LDA}(s_w)$ while s_w is in the range of [0,1]; this is the LDA total energy when a 1-s_w electron is removed from (valence band) or s_w electron is added to (conduction band) the corresponding Wannier functions. At neutral charge, the original valence band Wannier functions are fully occupied (sw = 1) and conduction band Wannier functions are fully occupied (sw = 0). The calculation involves fixing one Wannier function, occupying it with s_w electron and then variationally changing the other M wave functions to minimize the total energy. Here, M = N for conduction band Wannier functions, and M = N-1 for valence band Wannier functions, and these M wave functions must be orthogonal to each other and orthogonal to the Wannier function. The conjugated gradient method can be used to variationally solve the M wave functions and hence obtain $E_{LDA}(s_w)$ and λ_w. More computational details can be found in Ref. 14.

In our previous work, we have use the WKM to calculate the bandgaps of 27 common semiconductors. We found that the typical bandgap error is in a few tenth of eV similar to that of the GW calculations.[14] We have also used WKM to calculate the band alignment between the organic molecules and Au substrate. It is also found that the WKM yields accurate band alignment compared with experiments.[17] At this stage, it is thus important to test more cases for the WKM, to find out its range of validations. In this work, we will test the bandgap calculations of 20 alkali halide crystals, all in rock salt structures. Compared to the 27 common semiconductors studied in Ref. 14, which mostly are covalent bond systems, the alkali halide represents one extreme case: the most ionic crystals. We found that the WKM produces accurate bandgaps for the alkali halides. We also compared our results to the G_0W_0 and HSE06[18,19] bandgaps.

The LDA, HSE06, and WKM calculations are all implemented in the PWmat[20,21] code which runs on graphics processing unit processors. NCPP-SG15-LDA pseudopotential[22,23] is used. The alkali halides are all in the rock salt structures. The experimental lattice constants are used (supplementary material). A $10 \times 10 \times 10$ Monkhorst – Pack k-point set was used for a bulk 2 atom primary cell LDA and HSE06 selfconsistency and band structure calculation. A plane wave basis set cutoff of 50 Ryd is used. The calculated LDA band structure is shown in Fig. 1 for LiCl.

We also carry out G_0W_0 calculation using the Vienna *ab initio* simulation package (VASP) code[3,24] using projector augmented wave method potential.[25,26] The plane-wave cut off energy is set to 520 eV to ensure the accuracy. The Brillouin zone is sampled by $6 \times 6 \times 6$ Monkhorst k-points.[27] The number of empty bands for the 2 atom cell is set to 480 (equivalent to the energy of 240 eV above the bottom of the conduction band). PBE wave function and eigen energies are used as the input for the G0W0 calculation.

The Wannier function is calculated using the Wannier.90 package, with the Bloch wave functions and band energies calculated by PWmat. $10 \times 10 \times 10$ k-points are used in the construction of the Wannier function ϕ_w.[28] To make the correction for the eigen energy of an eigen orbital ψ_i, it is important to ensure $\sum_w \langle \phi_w | \psi_i \rangle^2 = 1$. In other words, sufficient

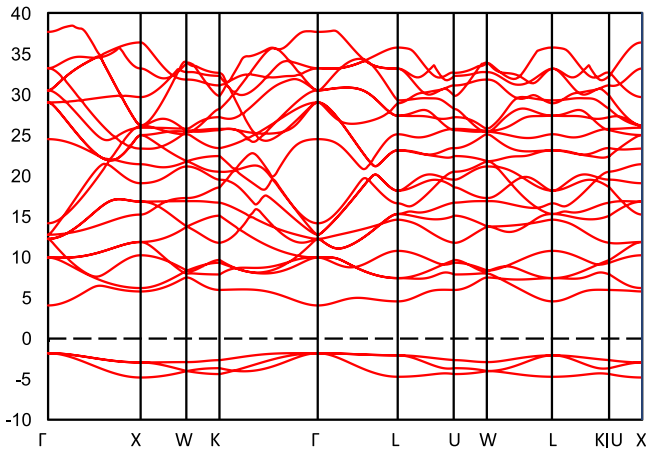

FIG. 1. LDA band structure of LiCl. The Fermi level is indicated by a dashed line.

TABLE I. The projections of Wannier functions on the VBM state of LiCl and the value of λ_w.

ϕ_w	$\lvert\langle\phi_w\lvert\psi_i\rangle\rvert^2$	λ_w (eV)
Cl-s	0.0000	2.37757
Cl-p_x	0.6630	1.85949
Cl-p_y	0.0000	1.85973
Cl-p_z	0.3370	1.86006
Li-s	0.0000	7.36524

Wannier functions are chosen to represent a Bloch state. For the valence band, we have used the s, p_x, p_y, and p_z states of the anion and the s state of the cation as the projectors to generate 5 orthogonal Wannier functions per primary cell as there are only 5 valence bands. Their projections to the VBM state are listed in Table I for the case of LiCl. The situation for the conduction band is more complicated; as can be seen in Fig. 1, there are no separated bands from the rest of the band structure. We have used the entangled band method[28] to construct the conduction band Wannier functions. In this method, two different energy windows are used. The Bloch states of the larger energy window are folded into the smaller energy window, and the generated Wannier functions are guaranteed to represent the Bloch states in the smaller energy window. However, this might result in a large number of Wannier functions (e.g., much more than 5 per atom in primary cell) as shown in Table II. However, we found that it is sufficient to use λ_w for only the first few Wannier functions with their projections to the conduction band minimum (CBM) state larger than 1%. One can renormalize the weight to 100%

TABLE II. The projections of Wannier functions on CBM of LiCl. The * indicates the sum of all the p Wannier functions or all the d Wannier functions. "a" indicates λ_w which is the average number of these orbitals.

ϕ_w	$\lvert\langle\phi_w\lvert\psi_i\rangle\rvert^2$	λ_w (eV)
Cl-s	0.9152	1.9205
Li-s	0.0837	1.2073
Li-p*	0.0009	1.4910[a]
Cl-p*	0.0002	1.6851[a]
Cl-d*	0.0000	1.5905[a]

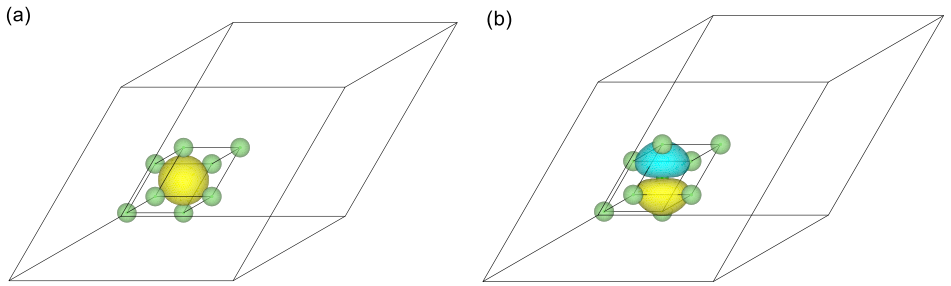

FIG. 2. (a) The Wannier function of Cl-px in the valence band and (b) the Wannier function of the Cl-s orbital in the conduction band.

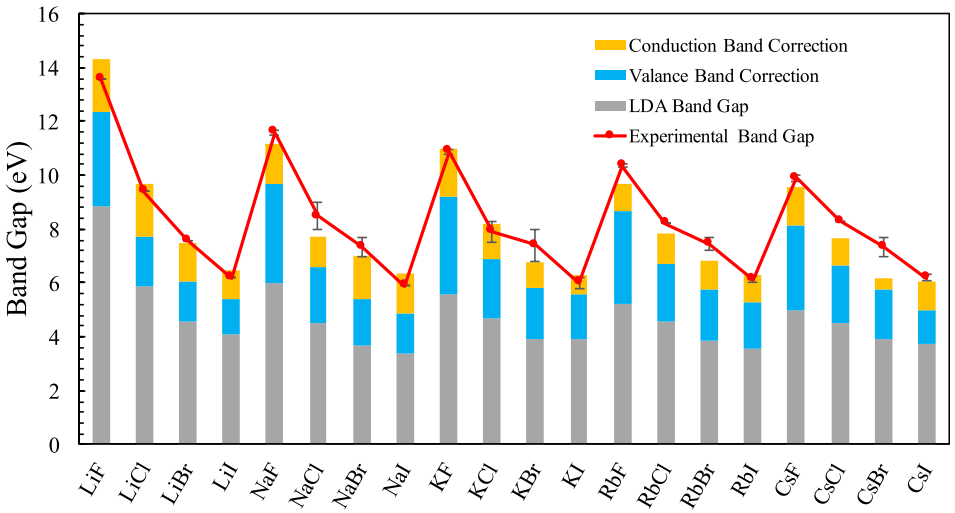

FIG. 3. The LDA bandgap and correction on the valence band and conduction band for WKM are shown in grey bar, blue bar, and orange bar, respectively. The red line shows the experimental bandgap, and the total height of the bar shows the WKM result. The error bar of the experimental bandgap showed the difference between different experimental results.[31,32]

after such a truncation. We found that the error induced is less than 10 meV and thus can be ignored. In this way, only λ_w of the two s state Wannier functions needs to be calculated. The Wannier function projections and their λ_w for all the 20 alkali halides are listed in Tables S3 and S4 of the supplementary material. A Cl-p state valence band Wannier function and a Li-s state conduction band Wannier function are shown in Fig. 2. We can see that they are both highly localized.

The calculation of λ_w for a given Wannier function is done in a supercell, much as for a charged point defect calculation. The details of such calculations can be found in Ref. 14. Following our previous work, a 128 atom supercell is used. We have also tested a 250 atom supercell for the LiCl system; the difference of λ_w in the conduction band between the results of 128 atoms is 0.13 eV, consistent with previous conclusions for other systems in Ref. 14. The obtained λ_w values are shown in Tables I and II as well as in Table S1 (supplementary material). As one can see, a typical λ_w is in the order of 1 eV.

After λ_w and the Wannier function projection to the Bloch band states are obtained, one can readily solve the modified eigen energy from Eq. (2). In the case of the Rock Salt crystal, the additional term of Eq. (2) will not cause any band mixing. As a result, the new eigen energy is simply $\varepsilon_i^{WKM} = \varepsilon_i^{LDA} + \sum_w \lambda_w \langle \phi_w | \psi_i \rangle^2$, and $\langle \phi_w | \psi_i \rangle^2$ is the projection as listed in Tables I and II. The eigen energy corrections are shown in Fig. 3. We see that roughly two thirds of the corrections come from the valence band, while one third is from the conduction band. For example, the VBM Wannier function corresponding to F, Cl, and Br is around 3.5, 1.8, and 1.5 eV, while the CBM Wannier function corresponding to cations Li, Na, and K is roughly1.8, 1.4, and 1.0 eV (although the actual number also depends on the anions). This λ_w difference mostly comes from the localization differences of the Wannier functions. In general, we found that the occupied Wannier functions are more localized than the unoccupied conduction band Wannier functions. This trend of more valence band correction is also found in methods like HSE and GW calculations. Finally, the calculated bandgaps compared to the experiments are shown in Fig. 4. In Fig. 4, we have also included the results from the G_0W_0 calculation and HSE06 calculation. In the HSE06, we have used the following standard parameters: alpha = 0.25 and

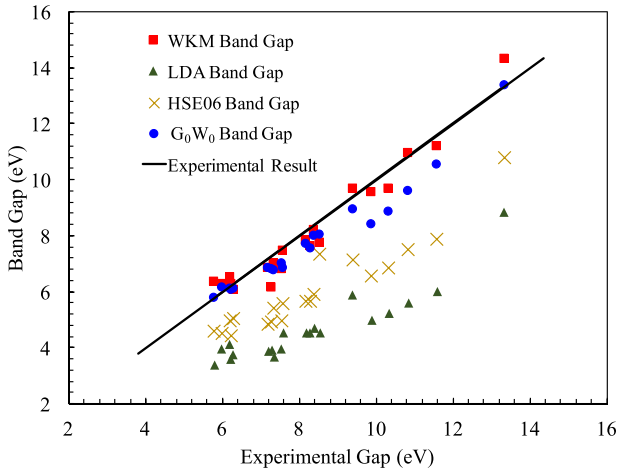

FIG. 4. The comparison of the WKM bandgap and other calculated bandgaps against experimental bandgaps of 20 alkali halide materials MX (M= Li, Na, K, Rb, and Cs; X = F, Cl, Br, and I). The HSE06 has a mixing parameter of $\alpha = 0.25$. The numbers of the figure can be found in Table S6 (supplementary material).

omega = 0.1058,[9,29] which work well in terms of correcting the common semiconductor bandgaps. However, as we can see, the HSE06 with these parameters significantly underestimates the bandgap. One can of course increase the value of alpha to have a better agreement with the experiment but that will make the parameter material dependent. On the other hand, the G_0W_0 with LDA as inputs yields much better agreement with the experiments. In general, the WKM results are of similar quality to the G_0W_0 results. The mean average deviation (MAD) of the WKM bandgap is 0.45 eV; for G_0W_0, it is 0.56 eV, for HSE it is 2.28 eV, and for LDA it is 3.63 eV.

Finally, it is worth noting that several recent works[30] indicate that the electron-phonon coupling can reduce the bandgap by a few tenth of an eV. It is shown in Ref. 30 that for LiF, the bandgap can be reduced by as much as 0.58 eV. For heavier element systems, such correction might be smaller. Nevertheless, such correction is still within the range of our WKM bandgap errors shown in Fig. 4, as well as the finite supercell size error shown in Ref. 14, and thus might not likely to alter our conclusion. Nevertheless, future investigation with higher accuracy calculations including effects like the electron-phonon couplings will be very interesting.

In conclusion, we have shown that the WKM can be used to calculate the highly ionic alkali halide crystals, and the calculated bandgap is in par with the G_0W_0 method and much better than the hybrid HSE06 method. We thus expect a wide usability of the WKM in terms of predicting the crystal band structures.

See supplementary material for details in WKM calculation of alkali halides.

The work was financially supported by the National Materials Genome Project of China (2016YFB0700600), the National Natural Science Foundation of China (Nos. 21603007 and 51672012), and Shenzhen Science and Technology Research Grant (Nos. JCYJ20150729111733470 and JCYJ20151015162256516). Wang was also supported by the Director, Office of Science (SC), Basic Energy Science (BES), Materials Science and Engineering Division (MSED), of the U.S. Department of Energy (DOE) under Contract No. DE-AC02-05CH11231 through the Materials Theory program (KC2301).

[1]J. P. Perdew and M. Levy, Phys. Rev. Lett. **51**, 1884 (1983).
[2]W. Kohn and L. J. Sham, Phys. Rev. **140**, A1133 (1965).
[3]G. Kresse and J. Furthmüller, Comput. Mater. Sci. **6**, 15 (1996).
[4]Y. Zhao and D. G. Truhlar, J. Chem. Phys. **125**, 194101 (2006).
[5]J. Sun, A. Ruzsinszky, and J. P. Perdew, Phys. Rev. Lett. **115**, 36402 (2015).
[6]J. Sun, R. C. Remsing, Y. Zhang, Z. Sun, A. Ruzsinszky, H. Peng, Z. Yang, A. Paul, U. Waghmare, X. Wu, M. L. Klein, and J. P. Perdew, Nat. Chem. **8**, 831 (2016).
[7]P. J. Stephens, F. J. Devlin, C. F. Chabalowski, and M. J. Frisch, J. Phys. Chem. **98**, 11623 (1994).
[8]K. Kim and K. D. Jordan, J. Phys. Chem. **98**, 10089 (1994).
[9]J. Heyd, G. E. Scuseria, and M. Ernzerhof, J. Chem. Phys. **118**, 8207 (2003).
[10]L. A. Constantin, E. Fabiano, and F. Della Sala, J. Chem. Theory Comput. **9**, 2256 (2013).
[11]M. S. Hybertsen and S. G. Louie, Phys. Rev. Lett. **55**, 1418 (1985).
[12]L. I. Bendavid and E. A. Carter, in *First Princ. Approaches to Spectroscopic Properties of Complex Mater.*, edited by C. Di Valentin, S. Botti, and M. Cococcioni (Springer, Berlin/Heidelberg, 2014), pp. 47–98.
[13]H. Cao, Z. Yu, P. Lu, and L.-W. Wang, Phys. Rev. B **95**, 35139 (2017).
[14]J. Ma and L.-W. Wang, Sci. Rep. **6**, 24924 (2016).
[15]C.-G. Zhan, J. A. Nichols, and D. A. Dixon, J. Phys. Chem. A **107**, 4184 (2003).
[16]J. F. Janak, Phys. Rev. B **18**, 7165 (1978).
[17]J. Ma, Z. F. Liu, J. B. Neaton, and L.-W. Wang, Appl. Phys. Lett. **108**, 262104 (2016).
[18]A. V. Krukau, O. A. Vydrov, A. F. Izmaylov, and G. E. Scuseria, J. Chem. Phys. **125**, 224106 (2006).
[19]J. Heyd and G. E. Scuseria, J. Chem. Phys. **121**, 1187 (2004).
[20]W. Jia, Z. Cao, L. Wang, J. Fu, X. Chi, W. Gao, and L. W. Wang, Comput. Phys. Commun. **184**, 9 (2013).
[21]W. Jia, J. Fu, Z. Cao, L. Wang, X. Chi, W. Gao, and L. W. Wang, J. Comput. Phys. **251**, 102 (2013).
[22]D. R. Hamann, Phys. Rev. B **88**, 085117 (2013).
[23]M. Schlipf and F. Gygi, Comput. Phys. Commun. **196**, 36 (2015).
[24]G. Kresse and J. Furthmüller, Phys. Rev. B **54**, 11169 (1996).
[25]P. E. Blöchl, Phys. Rev. B **50**, 17953 (1994).
[26]G. Kresse, Phys. Rev. B **59**, 1758 (1999).
[27]J. D. Pack and H. J. Monkhorst, Phys. Rev. B **16**, 1748 (1977).
[28]I. Souza, N. Marzari, and D. Vanderbilt, Phys. Rev. B **65**, 35109 (2001).
[29]J. Heyd, G. E. Scuseria, and M. Ernzerhof, J. Chem. Phys. **124**, 219906 (2006).
[30]G. Antonius, S. Ponce, E. Lantagne-Hurtubise, G. Auclair, X. Gonze, and M. Cote, Phys. Rev. B **92**, 085137 (2015).
[31]K. Teegarden and G. Baldini, Phys. Rev. **155**, 896 (1967).
[32]R. T. Poole, J. G. Jenkin, J. Liesegang, and R. C. G. Leckey, Phys. Rev. B **11**, 5179 (1975).